

CHAPTER 114

WAVE FORCES ON CROWN WALLS

Jan Pedersen¹

Hans F. Burcharth²

Abstract

This paper presents some of the results from a large parametric laboratory study including more than 200 long-duration model tests. The study addresses both the wave forces imposed on the breakwater crown wall as well as the performance of the structure in reducing the wave overtopping. The testing programme includes variations of the sea state parameters and of the geometrical configuration of the breakwater and crown wall. Basic relations between forces/overtopping and the varied parameters are examined and preliminary design guidelines for structures within the tested range of variations are proposed.

Introduction

A rubble mound breakwater is very often constructed with a crown or parapet wall at its crest, since such a superstructure contributes to the effectiveness of the breakwater in reducing the amount of overtopping water. Furthermore, a wall will in most cases reduce the necessary crest height of the rubble structure and thereby decrease the amount of rubble material. The superstructure often functions also as service and traffic road.

Although crown walls are very popular and have been used worldwide for decades, there still does not exist any general applicable guidelines or design criteria for these structures. This is in sharp contrast to some of the other modes

¹Ph.D., Department of Civil Engineering, Aalborg University, Sohngaardsholmsvej 57, DK-9000 Aalborg, Denmark

²Prof. of Marine Civil Engineering, Department of Civil Engineering, Aalborg University, Sohngaardsholmsvej 57, DK-9000 Aalborg, Denmark

of failure for rubble mound breakwaters where today's design procedures includes fairly reliable calculations of the probability of failure within the lifetime of the structure, see fx. [2, Burcharth 1991a] and [3, Burcharth 1991b]. Such calculations requires as basis a well documented design equation which for example for failure of the main armour layer is fulfilled by the Hudson formula or the stability formulae by [10, v.d. Meer 1988]. The uncertainties related to existing general formulae for wave wall stability and overtopping are very large. The design of crown walls therefore relies on site specific hydraulic model studies or careful extraction and interpretation of the research results presented in the literature, see fx. [1, Bradbury et. al. 1988], [7, Jensen 1983] and [8, Jensen 1984].

Looking at the stability of the crown wall, several modes of failure have to be considered as shown in Fig. 1.

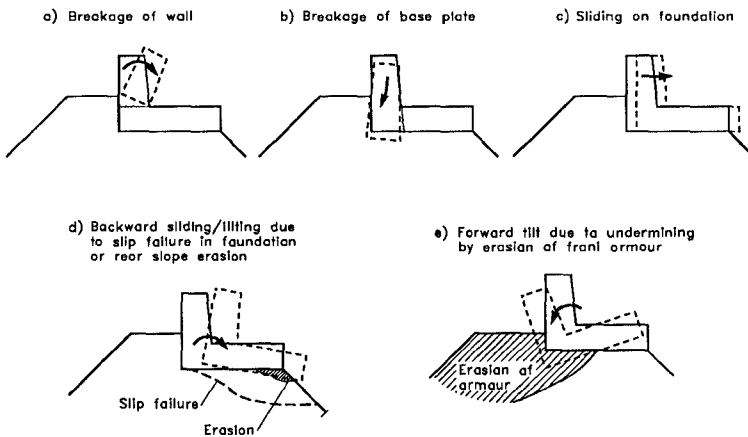


Fig. 1 - Possible failure modes for crown walls. From [4, Burchart 1993]

Only the failure modes a) and b) depends exclusively on the strength of the superstructure and the wave loading, whereas failure modes c), d) and e) are much more complex involving the properties of the underlying soil and failures of other parts of the structure. The problem of stability must in all cases be treated dynamically due to the dynamic behaviour of the wave loading. This imposes other problems since the transmissibility or relative amount of load transmitted to the rubble structure may be very different for the different failure modes. In the present investigations this dampening effect is not studied. All results relates to the pressures recorded on the stiff wave wall. The corresponding forces might be very conservative design measures especially for failure modes

c) and d), since these combined structure-soil failure mechanisms have relatively low transmissibility coefficients for short duration force actions. For a caisson breakwater [9, Oumeraci 1991] found a transmissibility coefficient in wave impact tests of 0.2-0.6 depending on the actual force history applied.

Model Tests

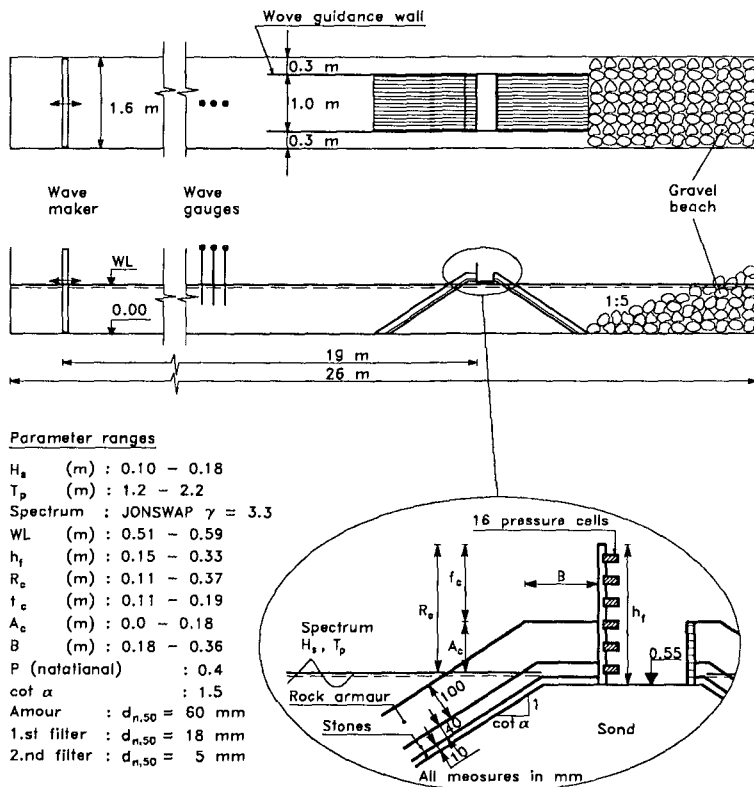


Fig. 2 - Experimental setup and parameter ranges.

Figure 2 shows the experimental setup used in the parametric laboratory study in one of the wave channels at Aalborg University. The channel is 1.6 m wide, 26 m long and is equipped with a piston type wave paddle. For the present study the wave channel was divided into a mid-section of 1 m width and two small side channels each of a width of 0.3 m. All varied parameters and their ranges

are given in Fig. 2. Waves are generated using a white noise filtering technique where it has been verified that the random number generator does not repeat itself, which is essentially for the probabilistic estimates of the measurements. Each of the over 200 performed test-runs consists of 4000-10000 waves, corresponding to 2-4 hours of run, in order to reach low exceedence probability levels with a high degree of reliability. Wave conditions are measured just in front of the breakwater and are separated in incident and reflected waves by a combination of the methods suggested by [6, Goda 1974b] and [5, Funke & Mansard 1980]. This separation is important since reflection amplitude coefficients of 20-30 % are registered.

The wave forces on the crown wall are measured using 16 Phillips P13 OEM 18 mm diameter pressure transducers mounted into the front face of the crown wall. In order to minimize the influence from local pressure disturbances the pressure cells are placed in 2-4 columns, dependent on the height of the used wave wall. Each column is displaced one diameter or less from the adjacent transducer columns, to get the best possible vertical resolution of the pressure field.

The wall itself consists of a 5 mm thick steel plate, supported several places along the width to ensure a stiffness large enough to prevent dynamic disturbances from movements and deformations. Preliminary tests using a strain gauge instrumented force table showed that this setup was unable to register the high frequent parts of the loading without introducing dynamic amplification and thereby blurring the measurements with signals from natural oscillations of the force table itself.

Sampling rates of 128 and 256 Hz were used depending on the actual geometric configuration. Only wave pressures on the front face of the wall were measured. The uplift pressure at the base plate was not recorded because of the uncertainty in correct scaling of the pore pressure in the underlying core material. Also, the forces from the armour units being in contact with the wall are not included in the present study.

From the pressure records the following force components (cf. Fig. 3) were calculated:

- The total horizontal force F_h .
- The base pressure P_b in the front base point.
- the overturning moment M_h around the front base point.
- The second order moment of pressures m_2 around the front base point.

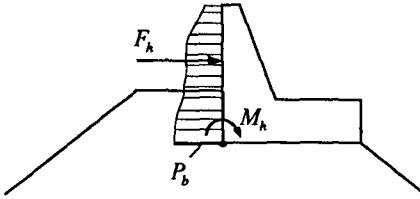


Fig. 3 - Calculated force components.

Forces

A typical example of the measured pressures on the crown wall is shown in Fig. 4. From left to right the figure illustrates the pressure evolution when a wave approaches the breakwater slope, hits the wall and starts to rush down. The timestep between each frame is 7.8 ms.

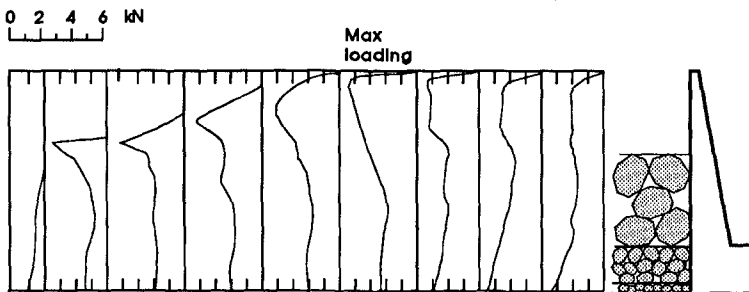


Fig. 4 - Example of typical pressure evolution on crown wall.
Timestep between each frame is 7.8 ms.

High local pressures are observed in a narrow region just above the crest of the armour in the same moment the water hits the wall. This phenomenon happens because the water velocities outside the porous stone layers are higher than inside. The maximum loading occurs a little later when the porous layers are fully saturated and the water pressure is acting over the full height of the wall. The pressure decay during the down-rush has a much longer duration (in the order of half a wave period) than the pressure rise which occurs within 0.02-0.05 seconds, i.e. in the order of 1-3 % of the wave period.

By spatial integration of the pressure recordings the horizontal force and the overturning moment are obtained. Examples of time series of these force

components are shown in Fig. 5, which also illustrates the afore mentioned time scales for pressure rise and decay.

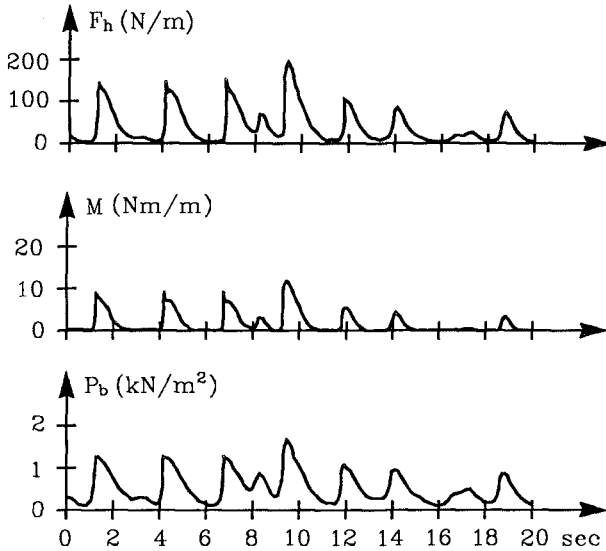


Fig. 5 - Examples of typical time series of force components. Obtained for lowest wall ($h_f = 0.15$ m).

For the further processing the time series are analysed and probabilistic estimates for each of the force components are extracted. For simplicity only $F_{0.1\%}$, being the horizontal force which has an exceedance probability of 0.1%, will be used in the following. Also, unless otherwise stated, all results discussed in the following are obtained for a high wall, where practically no overtopping occurs.

Influence of parameters

To represent the sea state conditions the significant wave height H_s and the spectral peak period T_p (or the corresponding wave length L_p) are used. For changes in water level [8, Jensen 1984] used the vertical distance A_c from the still water level to the armour crest and he showed that together with H_s it constitutes an important dimensionless parameter in predicting the wave forces on the crown wall. The influence of the width B of the armour crest and the height of the wave wall have also been examined. In Figs. 5-8 these different parameters are plotted against $F_{h,0.1\%}$.

Since the maximum forces are impulse forces (fig. 4 and 5) which are proportional to mv^2 , m being the mass of water hitting the structure and v the water velocity in the up-rush, which is proportional to \sqrt{gH} , it must be expected that the loading is proportional to H . The test results verify this, showing a clear linear dependency between H_s and $F_{h,0.1\%}$, Fig. 6. This is also in agreement with results by [1, Bradbury et. al 1988].

Like for H_s an increase in wave period and thereby wave length gives an increase in the wave load on the structure. Although the scatter is larger than for H_s Fig. 7 shows that the horizontal force is proportional to the wave length L_p . This result was also obtained by [8, Jensen 1984] whereas [1, Bradbury et. al 1988] found proportionality between the mean zero upcrossing wave period and the loading.

The parameter $\frac{H_s}{A_c}$, which incorporates variations in both wave height, water level and armour crest elevation, is in fig. 8 plotted against $F_{h,0.1\%}$, showing excellent linear dependency with nearly no scatter around the fitted lines.

In fig. 9 the results for different widths B of the crest berm are shown. Compared to the other investigated parameters, the influence of B is surprisingly small. As expected, the overall tendency is that the wave load on the wall decreases with increasing berm width, though when extending the width from $3d_{n,50}$ to $4d_{n,50}$ a small increase in the load is observed. No general conclusions of the influence of B on F can be drawn without examining the conditions for various force probability exceedence levels and various wave periods.

The last investigated parameter is the crown wall height h_f . From Fig. 10, where h_f is plotted against $F_{h,0.1\%}$ for five different values of $\frac{H_s}{A_c}$, it is seen that for small values of h_f and relative large values of $\frac{H_s}{A_c}$ an increase of the wall height results in an increase in the wave loading. Unfortunately, only two wall heights are situated in this part of the figure, but by using the point $(h_f, F) = (0,0)$ it is possible to get an idea of the relation between h_f and $F_{h,0.1\%}$. As seen in Fig. 10 this relation is quite non-linear. When the wave wall height is extended above a certain level, an upper limit, exclusively depending on sea state and water level, is reached. From this upper limit the wave force will no longer depend on h_f . For very low walls the influence of the sea state more or less vanishes and the horizontal force only depends on the height of the wave wall. This situation is caused by excessive overtopping where a large part of the up-rushing water spills over the structure without causing significant impulse loads.

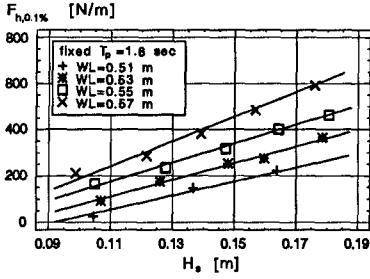


Fig. 6 - Influence of H_s

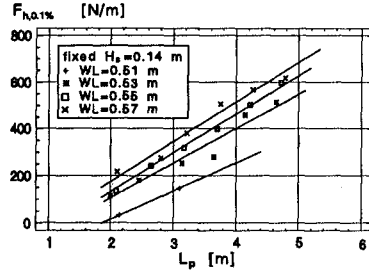


Fig. 7 - Influence of L_p

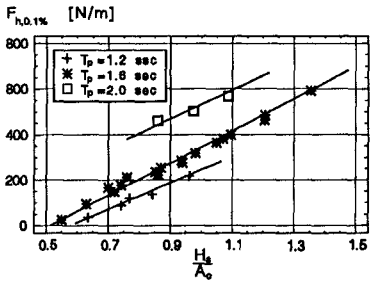


Fig. 8 - Influence of $\frac{H_s}{A_c}$

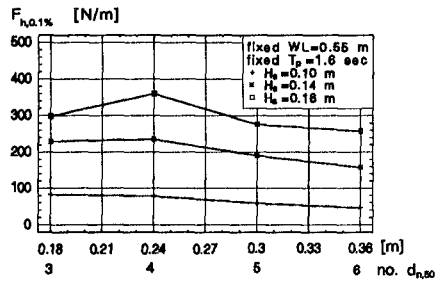


Fig. 9 - Influence of berm width B

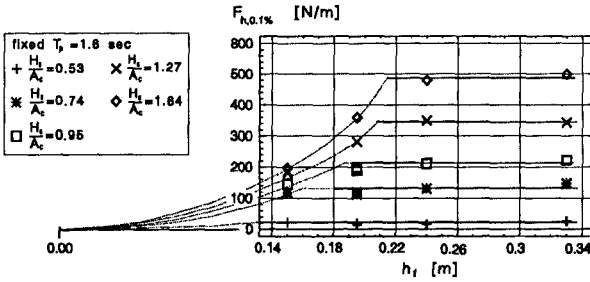


Fig. 10 - Influence of h_f

Guidelines for calculation of horizontal wave force

At present the only way to determine the horizontal wave loading on a crown wall accurately is by means of physical model tests. Based on such tests [8, Jensen 1984] proposed the following empirical relationship between $F_{h,0.1\%}$ and some of the parameters also examined in the present study :

$$\frac{F_{h,0.1\%}}{\rho g h_f L_p} = a \left(\frac{H_s}{A_c} + b \right) \tag{1}$$

where ρ is the water density and a and b are dimensionless empirical coefficients. Although the method by which the different parameters have been non-dimensionalised is not fully correct, the main features of the formula are verified by the current study. Figs. 6 and 7 show the same linear influence of H_s and L_p respectively as expressed in eq. 1. The influence of the wall height h_f however, which in eq. 1 also is expressed as proportional to F , can not be confirmed. Although slightly unreliable due to the relative few wall heights tested the current study shows that h_f should enter the formula in a power larger than 1. Assuming that the major part of the load is caused by hydrostatic water pressure, one finds that the horizontal force is a function of h_f^2 which, although the forces are merely caused by impact pressures, supports the present observations.

In Fig. 11 the ratio $\frac{H_s}{A_c}$ is plotted against the left hand side of equation 1 for model test results obtained from [8, Jensen 1984], [1, Brabury et. al 1988] and the present study.

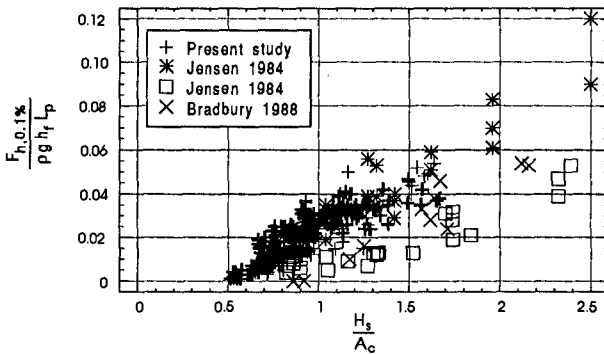


Fig. 11 - Different model test results plotted according to eq. 1.

Although not fully explaining the influence of all relevant parameters, and showing quite a lot of scatter compared to the model test results, eq. 1 still provides a satisfactory first estimate on the wave loading on the crown wall.

Overtopping

In all model tests performed also the mean overtopping rate Q_m was measured. An 0.5 m wide tank for collection of the water discharged over the crown wall was installed in the middle of the test section and fitted to the top of the wall. From the tank the water was automatically pumped through a flow meter and back into the flume. Reading of the flow meter was taken after each test. Fig. 12 illustrates the used setup.

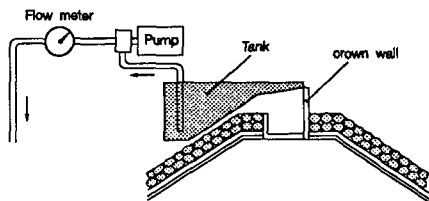


Fig. 12 - Sketch of setup for overtopping measurements.

Like for the study of the wave forces the overtopping results are used to examine the influence of the different sea state and geometrical parameters on Q_m .

Influence of parameters

Fig. 13 shows the significant wave height plotted against Q_m for fixed wave period, wall height and berm width but for different water levels. As seen the influence from H_s on Q_m is very large. Q_m is approximately proportional to H_s^5 . In Fig. 14 the influence of changes in water level and wall height is shown. R_c being the distance from the still water level to the top of the wave wall, is able to incorporate the variations of both parameters. The ratio $\frac{H_s}{R_c}$ is seen to constitute an important dimensionless parameter expressing the influence of both the wave height and the vertical distance to the top of the structure.

Several examinations of how the wave period alters Q_m were carried out, showing no general dependency for nor T_p or L_p . The ratio $\frac{L_m^2}{T_m^2}$ (or $c_m L_m$) where T_m is the mean zero upcrossing period and L_m and c_m the corresponding wave length and wave celerity, offers a very fine expression for the influence of the period cf. Fig. 15. This figure shows, with nearly no scatter around the fitted lines, that

Q_m depends linearly on $\frac{L_m^2}{T_m}$.

Finally also the influence of the armour berm width B on the mean overtopping rate has been investigated. As expected Fig. 16 shows that when B increases the amount discharged over the wall decreases. Q_m is approximately proportional to $\frac{1}{B}$.

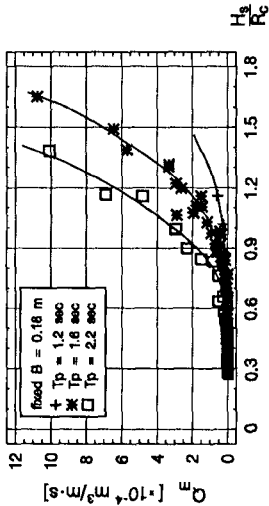


Fig. 14 - Influence of $\frac{H_s}{R_c}$

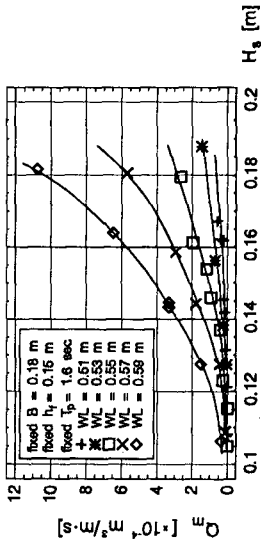


Fig. 13 - Influence of H_s

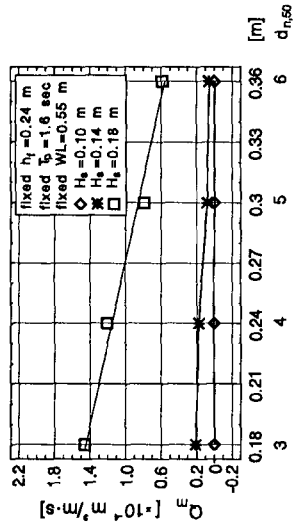


Fig. 16 - Influence of berm width B

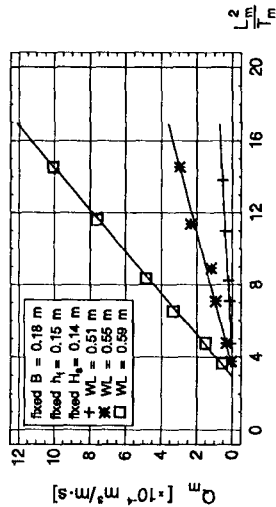


Fig. 15 - Influence of $\frac{L_m^2}{T_m}$

Guidelines for calculation of mean overtopping rates

Several researchers have studied the subject of overtopping of coastal structures. Probably the most comprehensive work concerning crown walls on rubble mound breakwaters is found in [1, Bradbury et. al 1988]. Based on a large model study the authors suggest the following expression for calculation of the mean overtopping rate :

$$Q^* = \alpha (F^*)^\beta \quad (2)$$

where

$$Q^* : \text{dimensionless discharge} = \frac{Q_m}{T_m g H_s}$$

$$F^* : \text{dimensionless freeboard} = \left(\frac{R_c}{H_s} \right)^2 \sqrt{\frac{s_p}{2\pi}}$$

α, β : empirical coefficients depending on breakwater
and wave wall geometries

In Fig. 17 $\ln(F^*)$ is plotted against $\ln(Q^*)$ for the model test results obtained in the present study. For all results shown the armour berm width was kept constant at 0.18 m ($3d_{n,50}$). Though some scatter is observed eq. 2 generally predicts the overtopping rates very well. For the actual case α and β was fitted to $7.4 \cdot 10^{-8}$ and -2.58 respectively.

Based on the analysis of the influence of the different examined parameters on Q_m (cf. Figs. 13-16) the following alternative relationship for prediction of the overtopping rates was developed :

$$\frac{Q_m T_m}{L_m^2} = \alpha \left(\frac{H_s}{R_c} \right)^\beta \quad (3)$$

where α and β are empirical dimensionless coefficients.

As in eq. 2 the influence of the armour berm width must be included in α and β , since a general non-dimensional expression for this parameter has not yet been found. Also, the effects of permeability, slope angle and slope roughness have to be included in α and β just as for eq. 2. In Fig. 18 logarithmic values of both sides of eq. 3 are plotted for a fixed armour berm width of 0.18 m ($3d_{n,50}$). Compared to Fig. 17 the scatter around the fitted line is a little smaller. α and β are fitted to $1.26 \cdot 10^{-5}$ and 5.2 respectively.

It must be concluded that both models, eq. 3 slightly better than eq. 2, are able to predict the amount of water overtopping the wave wall with quite good accuracy.

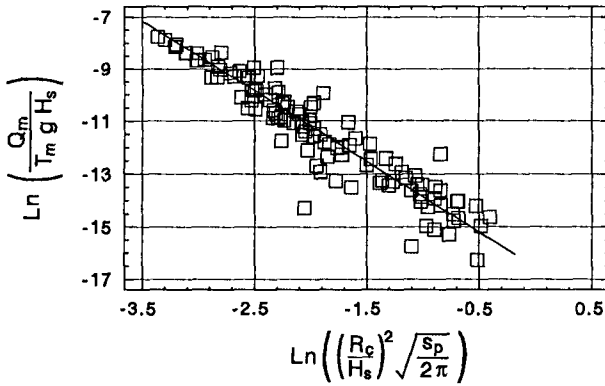


Fig. 17 - Plot of $\ln(F^*)$ against $\ln(Q^*)$ from eq. 2.

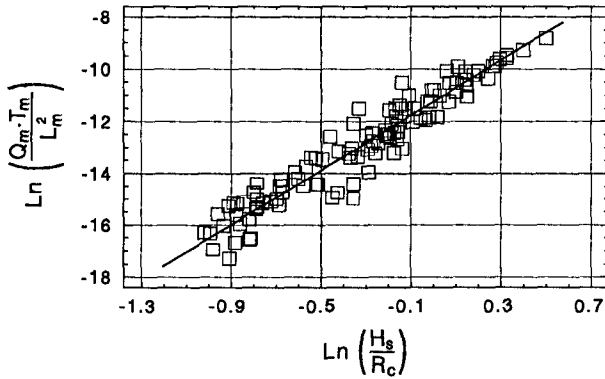


Fig. 18 - Plot of $\ln\left(\frac{Q_m T_m}{L_m^2}\right)$ against $\ln\left(\frac{H_s}{R_c}\right)$ from eq. 3.

Conclusions

Some of the results obtained from an extensive parametric model study concerning wave forces and overtopping on rubble mound breakwater crown walls have been presented.

The analyses more or less confirm the relationship suggested by [8, Jensen 1984] for prediction of the horizontal wave forces, though some discrepancies are observed. Until more work has been carried out on this subject the formula by

Jensen serves well as a first estimate in assessing the wave load.

Concerning wave overtopping a new formula has been developed, which, although not fully complete, is able to predict the mean overtopping rate on the wave wall with quite good accuracy. The relationship proposed by [1, Bradbury et.al] has also been analysed and shows an almost similar accuracy in estimating the amount of water discharged over the crown wall.

References

- [1] Bradbury A. P., N. W. H. Allsop, R. V. Stevens. *Hydraulic performance of breakwater crown walls*. Hydraulics Research, Wallingford, Report SR146, 1988.
- [2] Burcharth H. F. *Development of a partial coefficient system for the design of rubble mound breakwaters*. PIANC Working Group 12, Subgroup-F report, 1991.
- [3] Burcharth H. F. *Recommendation of a partial coefficient system for the implementation of predetermined safety in the design of rubble mound breakwaters*. PIANC, PTC II, Working Group 12 report, 1991.
- [4] Burcharth H. F. *The design of rubble mound breakwaters*. Aalborg University, In print, to be published, 1993.
- [5] Funke E. R., E. P. D. Mansard. *The measurement of incident and reflected spectra. Using a least squares method*. Proc. Coastal Engineering Conf., 1980.
- [6] Goda Y., Y. Suzuki. *Estimation of incident and reflected waves in random wave experiments*. Proc. Coastal Engineering Conf., Copenhagen, 1976.
- [7] Jensen O. J. *Breakwater superstructures*. Proc. Coastal Structures Conf., Arlington, 1983.
- [8] Jensen O. J. *A monograph on rubble mound breakwaters*. Danish Hydraulic Institute, 1984.
- [9] Oumeraci H. *Dynamic loading and response of caisson breakwaters - Results of large-scale model tests*. MAST G6-S, Project 2 research report, Franzius Institut, 1991.
- [10] van der Meer J. W. *Rock slopes and gravel beaches under wave attack*. Delft Hydraulics, 1991.